Agenzia Nazionale per le Nuove Tecnologie,
l'Energia e lo Sviluppo Economico Sostenibile

Ministero dello Sviluppo Economico

RICERCA DI SISTEMA ELETTRICO

Maximum pressure calculations at quench during cold test

G. M. Polli, U. Besi-Vetrella, A. Cucchiaro, L. Muzzi

Report RdS/2011/392

MAXIMUM PRESSURE CALCULATIONS AT QUENCH DURING COLD TEST

G. M. Polli, U. Besi-Vetrella, A. Cucchiaro, L. Muzzi (ENEA)

Novembre 2011

Report Ricerca di Sistema Elettrico
Accordo di Programma Ministero dello Sviluppo Economico – ENEA
Area: Governo, gestione e sviluppo del sistema elettrico nazionale
Progetto: Fusione nucleare: Attività di fisica e tecnologia della fusione complementari ad ITER, denominate "Broader Approach"
Responsabile Progetto: Aldo Pizzuto, ENEA

MAXIMUM PRESSURE CALCULATIONS AT QUENCH DURING COLD TEST

Rev. 0 20/04/2011

		L. Muzzi		
		A. Cucchiaro		
0	20/04/2011	U. Besi-Vetrella		
		G.M. Polli		
Rev.	Date	Author	Reviewer	Approver

Maximum pressure calculations at quench during cold test

by
G. M. Polli, U. Besi Vetrella, A. Cucchiaro, L. Muzzi

Abstract

The maximum pressure reached during quench simulations of the JT-60SA TF magnet in the foreseen cold test facility is reported. To drive the quench in the numerical simulations a field perturbation is used in the region where the maximum self field is located. Several cases are considered with different helium inlet conditions and delay times in order to identify the set of parameters for which the maximum pressure maintains below 20 bars.
In an annexed document a summary of the analyses carried out in 2008 to assess the quench behavior of the central pancake in the operative conditions is also reported.

Table of Contents

1 Outline

Several analyses have been carried out in the present study to determine the maximum pressure that will be reached during the cold test after a quench started. Whilst in the real situation the quench will be induced by the increase of the helium inlet temperature up to the current sharing temperature in the region of maximum self field, in the present calculations the quench has been driven by a square wave of field disturbance in the region of maximum field. Specifically, the disturbance has an extension of 0.5 m and lasts in 0.5 s (see Table 2 for the intensity) and it is located where the maximum self field is reached. This choice has been done to avoid the use of external heat input components to be deposited in the conductor, which would not be present during the cold test, where the quench is induced by slowly increasing the He inlet temperature up to current sharing.

The self field distribution along the first layer and across the equatorial plane of the central pancake of the winding pack (WP), provided in [1] using Opera 3D code, has been used as an input in the 1D thermo-hydraulic analyses carried out with Gandalf code. Figure 1 shows the self field distribution employed in Gandalf at the instant of time when the field perturbation starts (1000.25 s). The curve shows the exact variation between each layer based on the mean value in the conductor cross section.

Figure 1 Distribution of magnetic field self-induced in the WP during cold test

Table 1 reports the nominal operative conditions that are foreseen during the tests in the cold test facility.

Table 1 Nominal operative conditions in the cold test facility

Property	Value
He inlet temperature [K]	7.5
He inlet pressure [bar]	7.0
He outlet pressure [bar]	>4.5
He mass flow rate [g/s]	2.0
Delay time [s]	2.0
Discharge time [s]	10.0
Voltage threshold [V]	0.1

2 Results

Table 2 shows the summary of the analyses carried out to perform the present study. Six parameters have been varied one at a time in order to measure their influence on the maximum pressure reached after the quench started. The parameter varied passing from one case to the following is highlighted in boldface and italics. In the table also the outlet pressure and the maximum pressure, where the field disturbance is located and, at x=70 m from inlet, where the maximum pressure is reached, are shown. Note that in all the considered cases, the inlet pressure and mass flow were input data for the code.

Table 2 Summary of the carried out analyses

Case #	resid time [s]	P inlet [bar]	T inlet [K]	MFR [g/s]	delay time [s]	discharge time [s]	B max [T]	DB/ B [%]	P outl. [bar]	P_max @ x=15m [bar]	P_max @ x=70m [bar]
01	339.	7.0	7.0	4.0	2.0	10.0	4.0	26%	5.6	32.7	44.1
02	678.	7.0	7.0	***2.0***	2.0	10.0	4.0	26%	6.6	33.6	46.7
03	678.	7.0	7.0	2.0	2.0	10.0	***3.8***	20%	6.6	33.6	46.7
04	678.	7.0	7.0	2.0	***1.0***	10.0	3.8	20%	6.6	31.0	41.5
05	497.	***5.4***	7.0	2.0	***2.0***	10.0	3.8	20%	4.9	25.6	34.8
06	497.	5.4	7.0	2.0	***1.0***	10.0	3.8	20%	4.9	23.9	31.1
07	791.	5.4	***6.0***	2.0	1.0	10.0	***6.3***	99%	5.1	11.6	7.3
08	751.	***8.0***	***7.0***	2.0	1.0	10.0	***3.8***	20%	7.6	33.8	45.7
12	454.	***5.4***	***7.2***	2.0	1.0	***5.0***	***3.3***	***5%***	4.9	22.2	22.3 (24.1)
13	632.	***7.0***	7.2	2.0	1.0	5.0	3.3	5%	6.6	29.2	30.6 (32.0)

Note that in all the cases with 10 s of discharge time, except for case #07, the maximum pressure exceeds 30 bar. Conversely, in the cases with 5 s of discharge time the maximum pressure is close or below 30 bars.[1] Note also that the maximum pressure in cases #12 and #13 is neither at 15 m or at 70 m from the inlet but it is even reported in the last column in brackets.

2.1 Nominal discharge time (10 s)

Limited to cases with 10 s of discharge time, a possible explanation of the different behavior encountered in these calculations can be derived from Figure 2.

[1] The nomenclature of the cases with 5 s of discharge time is not consecutive with respect to those with 10 s because other cases, not reported here, have been analyzed in between.

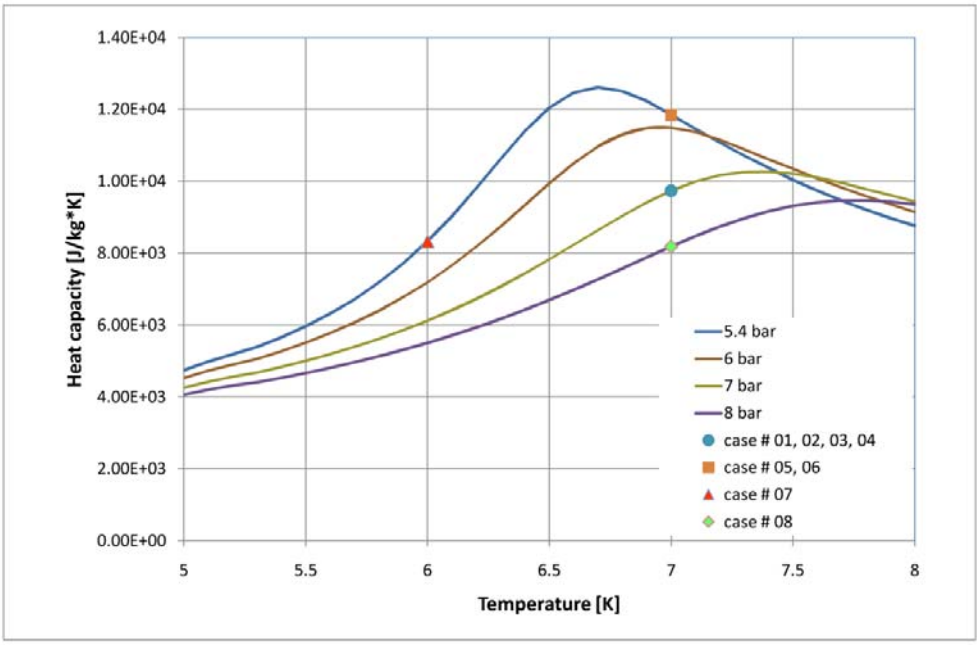

Figure 2 Helium specific heat capacity as a function of the temperature at different pressures

In this figure the helium specific heat capacity at the different pressure is plotted as a function of the temperature. Also the characteristic points of the 8 studied cases are identified in the figure. It is apparent that in case 07 the helium is located in a region of higher thermal stability ($dc_p/dT > 0$) and it has 1.5K before reaching its maximum. This feature translates into a greater ability to absorb heat in the instants following the start of the quench when the current has not yet been reduced.
More specifically the amount of energy that could be absorbed by the helium in the conductor before it quenches is given by the integral of the specific heat between the reference temperature and the Tcs (~7.5 K), multiplied by the mass of helium (that depends on the reference temperature). Table 3 reports the energy margin, that is the amount of energy that can be released without quench starting, in the different cases analyzed.

Table 3 Energy margin before quench [J]

P_ref =5.4 bar T_ref =6 K	P_ref =6 bar T_ref =7 K	P_ref =7 bar T_ref =7 K	P_ref =8 bar T_ref =7 K
2.62E+04	6.25E+03	6.81E+03	6.57E+03

As recalled in the outline, the thermo-hydraulic calculations have been performed using Gandalf 1D code[2]. Analyses have been divided into two steps. First a steady state condition have been reached then a transient analysis has been conducted with the field perturbation. Note that the steady state step lasts 1000 s since the longest residence time among those expected in the different cases is 791 s as shown in Table 2.
Since the pressure reached in the steady state at the boundaries is maintained during the transient, it happens that a reverse mass flow appears at the inlet and an increase of mass flow at the outlet after the quench started. These effects, highlighted in Figure 3 and Figure 4, can

[2] For conservative reasons, in the Gandalf input, the maximum content of copper among those allowed in the strand specifications (i.e. Cu/nCu=1.9) has been considered to estimate the area of NbTi and that of copper material within the cable.

be interpreted as a sort of security valves that evacuates the excess of helium to maintain the requested pressure. In particular, Figure 3 refers to case #4 whereas Figure 4 to case #7.

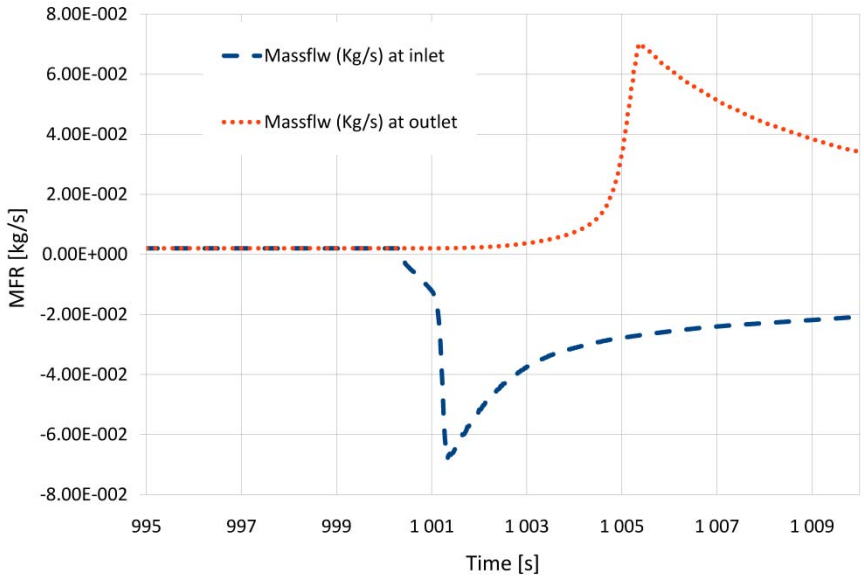

Figure 3 Mass flow rate evolution at inlet and outlet in the case #4

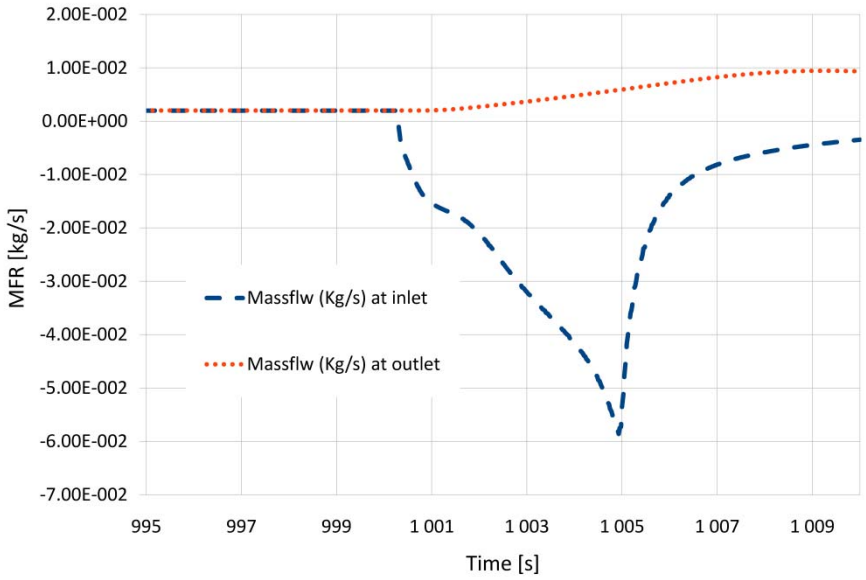

Figure 4 Mass flow rate evolution at inlet and outlet in the case #7

Regarding the evolution of the pressure within the pancake Figure 5 and Figure 6 show the pressure time histories in the place where the field perturbation is located (x=15m) and at x=70 m in the case #4 and #7.

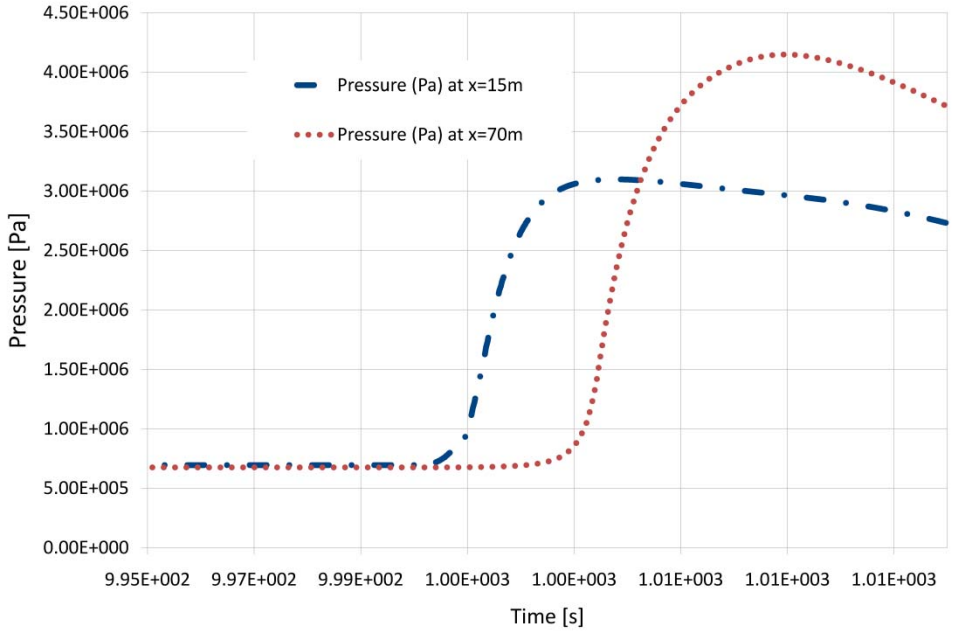

Figure 5 Pressure evolution where the quench initiates (x=15m) and where reaches its maximum (x=70m) in case #4

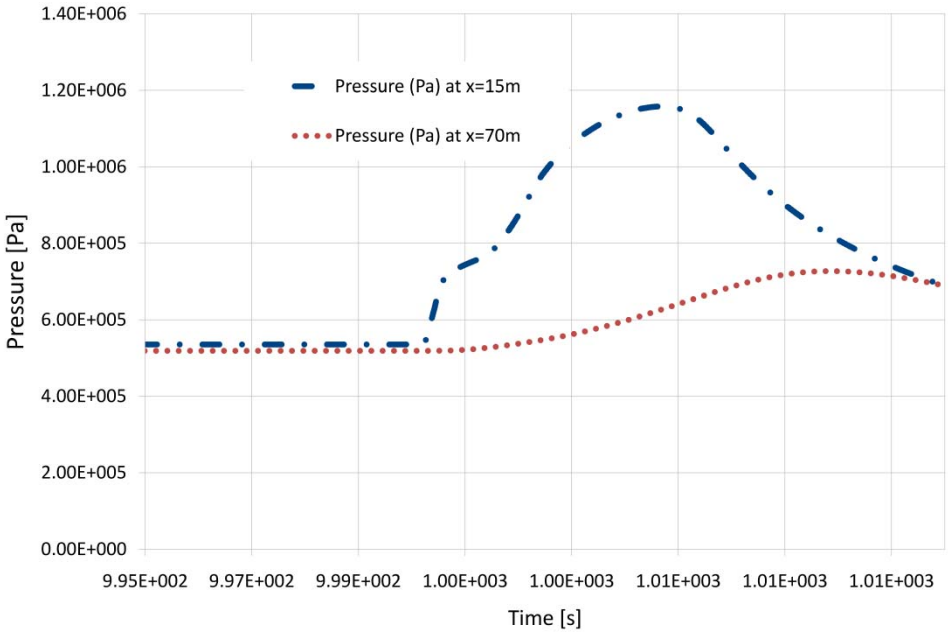

Figure 6 Pressure evolution where the quench initiates (x=15m) and where reaches its maximum (x=70m) in case #7

Pressure distribution within the pancake and its evolution are plotted also in Figure 7 and Figure 8 for the two cases examined (#4 and #7).

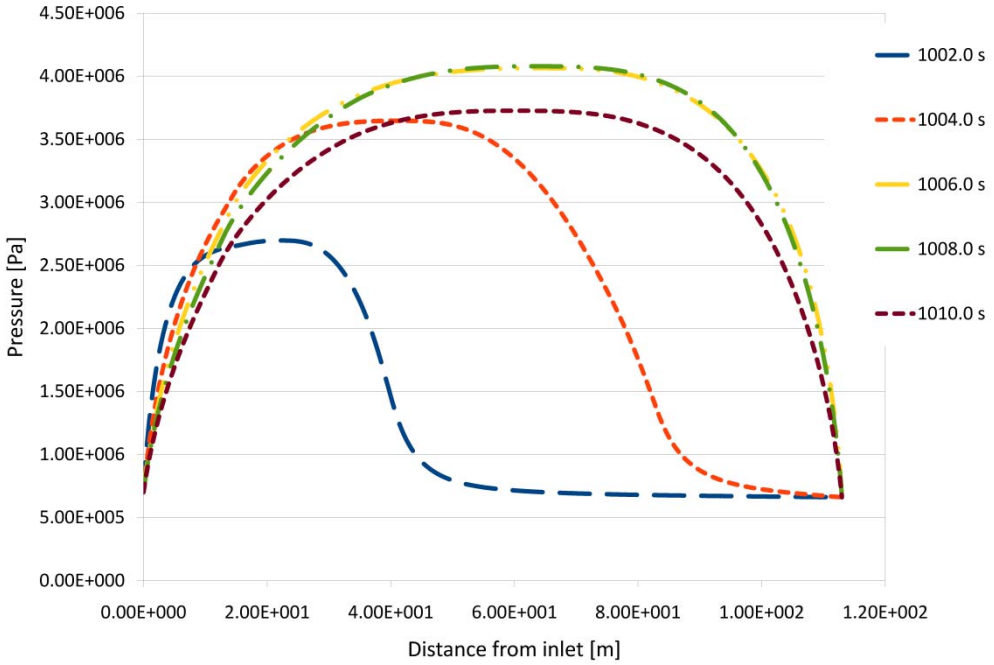

Figure 7 Pressure distribution within the central single pancake at different instant of time after quench initiation in case #4.

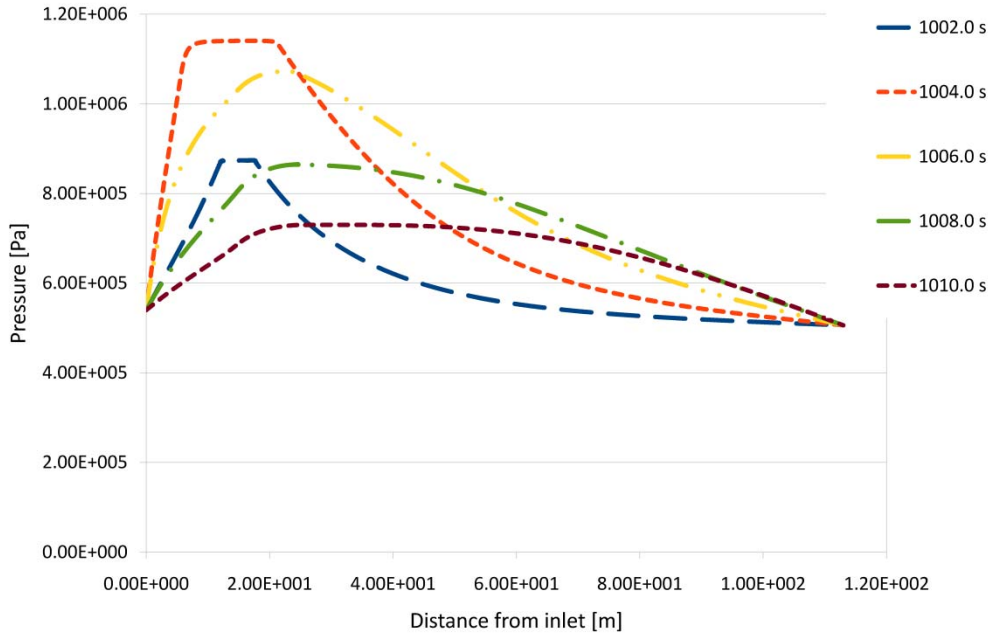

Figure 8 Pressure distribution within the central single pancake at different instant of time after quench initiation in case #7

2.2 Reduced discharge time (5 s)

As soon as the discharge time is halved (from 10 to 5 s) a significant reduction in the maximum pressure can be found (see Table 2). The two cases reported differ with respect to the others not only for the discharge time but also for the field perturbation considered to

drive the quench (5 instead of 20% increase) and for an inlet temperature closer to the current sharing temperature of the conductor (7.2 instead of 7.0 K).[3]
The following figures show the pressure evolution within the central pancake in the two cases with 5 s of discharge time.

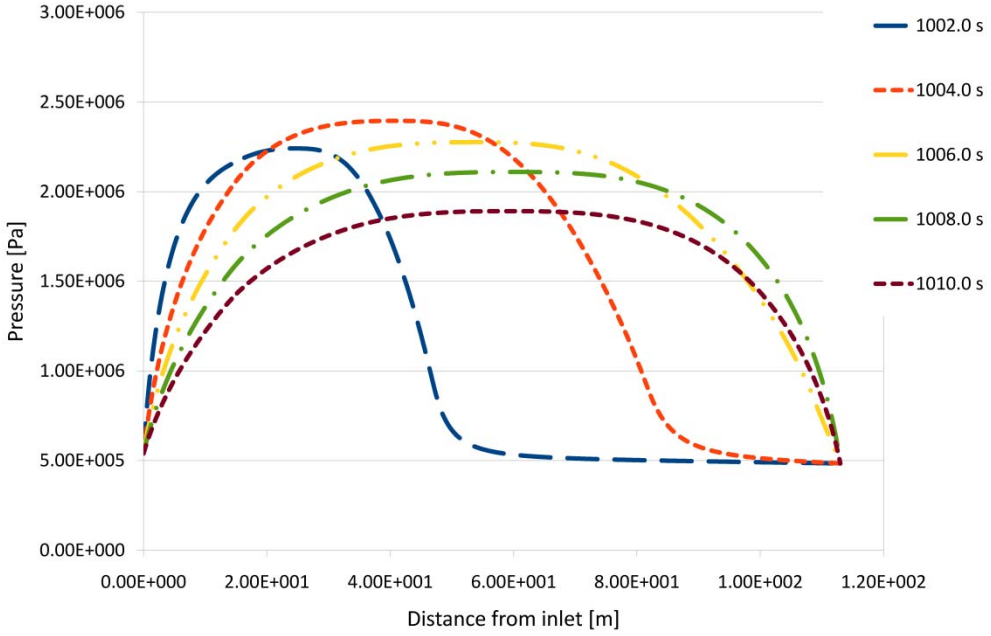

Figure 9 Pressure distribution within the central single pancake at different instant of time after quench initiation in case #12

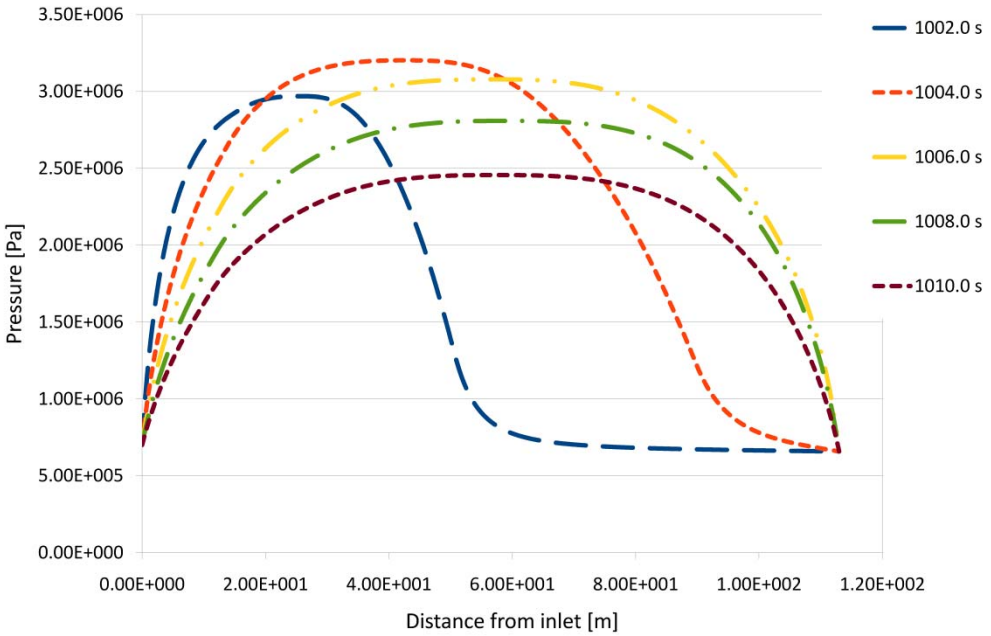

Figure 10 Pressure distribution within the central single pancake at different instant of time after quench initiation in case #13

[3] In other cases, not shown here, the effect of the way to induce the quench (DB=20% & T=7.0 K) has been analyzed and no practical difference in the maximum pressure has been noted with respect to the cases here reported (DB=5% & T=7.2 K) .

3 Summary and conclusions

The maximum pressure in the TF JT-60SA central pancake has been calculated at quench during the cold test. In almost all the conditions studied the maximum pressure exceeded the 30 bar, and neither the reduction of pressure inlet or the halving of the delay time have been sufficient to lower the max pressure under 20 bar. Only the reduction of the discharge time and the decrease of the inlet pressure determined a significant reduction of max pressure around 20 bar. Further reduction could be obtained by decreasing the inlet temperature and driving the quench through an external 3T perturbation of magnetic field.

References

[1] S. Turtù, private communication.

Annex A: Past simulations of quench during normal operations

Quench simulations, by Gandalf, of JT-60SA TF magnet during operation

In November 2008, ENEA performed thermo-hydraulic simulations of quench events in the JT-60SA TF magnets inside the tokamak during operation, using the 1-D code Gandalf. The computations were aimed at assessing whether the assumed value for the delay time constant (τ_{delay} = 2s) could be considered as an acceptable value for quench detection (+ opening of switches and breakers), or whether quenches developed too slowly to be reliably detected within this timeframe. At the same time, from these simulations the maximum value of pressure inside the conductor at quench could be inferred.
For these analyses, a set of disturbance scenarios has been considered, parametrically varying the main features of the heat input driving the quench, i.e. either varying the heated conductor length, or the disturbance duration, as well as its maximum energy.
All simulations have been carried out with an inlet temperature T_{inlet}=4.6K; and with P_{inlet}=6bar – P_{outlet}=5 bar. The complete magnetic field profile along the conductor length, is considered in the simulations.

Case	Disturbance length	Disturbance duration	Input power for quench	Input energy for quench	Time to reach quench detection threshold (V=100mV)
	ΔL (m)	Δt (s)	Q (W/m)	Q (J)	t(ms)
1	1	1	200	200	350
2	10	1	200	2000	400
3	0.1	1	200	20	800
4	1	0.01	10000	100	200
5	10	0.01	10000	1000	< 100

The following table summarizes the set of results, for the different scenarios studied. In the worst case scenario (case 3, corresponding to the slowest quench evolution), the voltage on the coil after quench reached the quench detection threshold ($V_{threshold}$ = 100 mV) after 800 ms.

Taking, as an example, the case #3, the **maximum pressure** during quench has been found to be $\mathbf{P_{max}}$ **= 20 bar**, and corresponding to a maximum temperature $\mathbf{T_{max}}$ **= 55K** (see following plot).

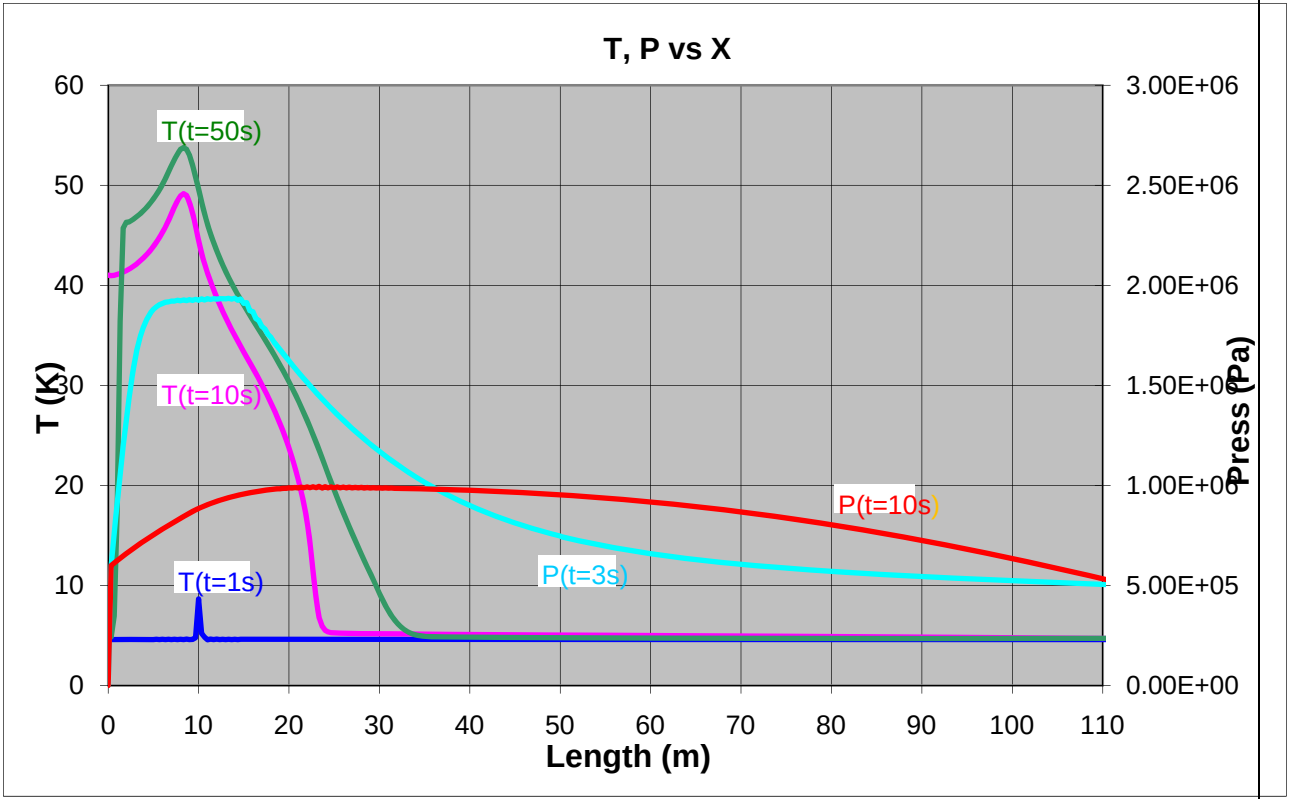

Annex B: Quench propagation speed

The following plot shows the propagation speed (defined as time derivative of the total normal length) for cases #03,05 and 07 of Table 2.

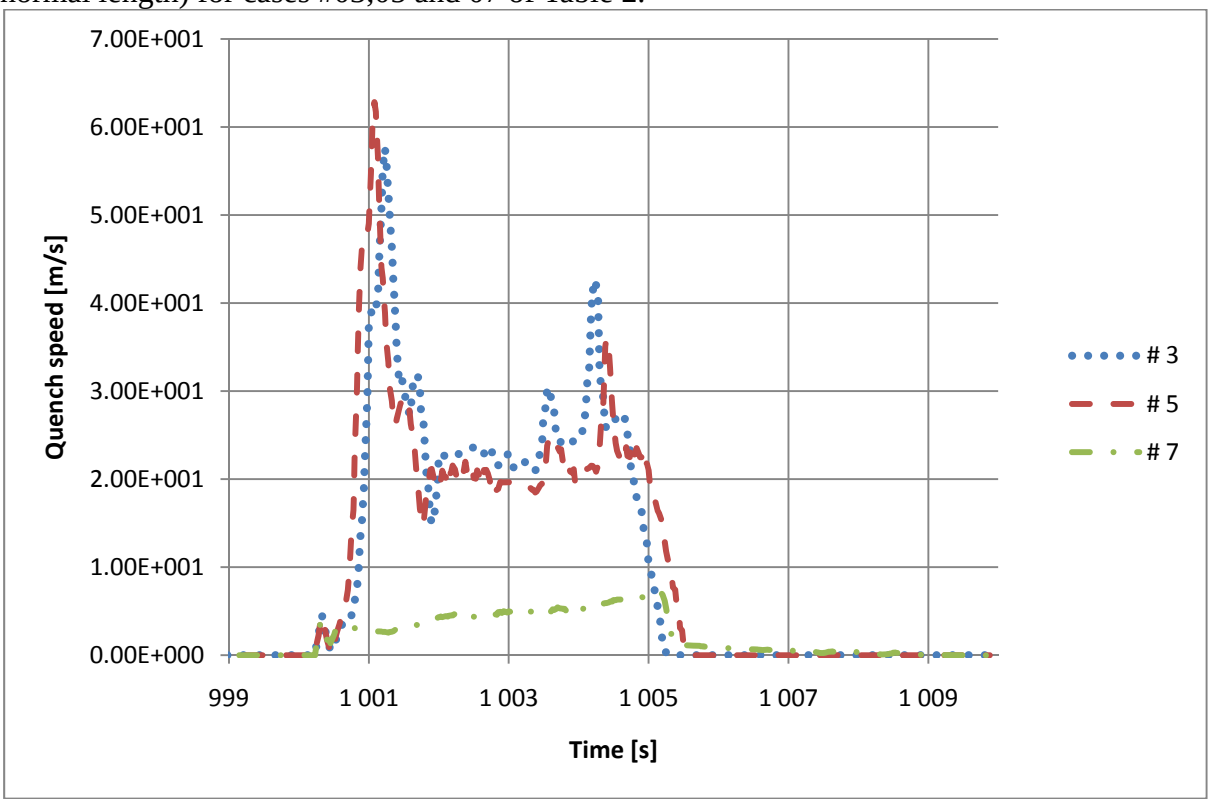

Maximum quench speed during the quench evolution are listed in the following table.

Case	Max speed [m/s]
03	57.6
05	62.8
07	7.1